European Journal of Radiology Open 3 (2016) 182–190

European Journal of Radiology Open

journal homepage: www.elsevier.com/locate/ejro

Intra-individual diagnostic image quality and organ-specific-radiation dose comparison between spiral cCT with iterative image reconstruction and z-axis automated tube current modulation and sequential cCT

Holger Wenz[a,*], Máté E. Maros[a], Mathias Meyer[b], Joshua Gawlitza[b], Alex Förster[a], Holger Haubenreisser[b], Stefan Kurth[a], Stefan O. Schoenberg[b], Christoph Groden[a], Thomas Henzler[b]

[a] Department of Neuroradiology, University Medical Center Mannheim, Medical Faculty Mannheim, Heidelberg University, Germany
[b] Institute of Clinical Radiology and Nuclear Medicine, University Medical Center Mannheim, Medical Faculty Mannheim, Heidelberg University, Germany

ARTICLE INFO

Article history:
Received 31 May 2016
Accepted 31 May 2016
Available online 26 July 2016

Keywords:
Spiral cranial CT
Sequential cranial CT
Iterative reconstruction
Automatic tube current modulation
Organ-specific-radiation dose

ABSTRACT

Objectives: To prospectively evaluate image quality and organ-specific-radiation dose of spiral cranial CT (cCT) combined with automated tube current modulation (ATCM) and iterative image reconstruction (IR) in comparison to sequential tilted cCT reconstructed with filtered back projection (FBP) without ATCM.
Methods: 31 patients with a previous performed tilted non-contrast enhanced sequential cCT aquisition on a 4-slice CT system with only FBP reconstruction and no ATCM were prospectively enrolled in this study for a clinical indicated cCT scan. All spiral cCT examinations were performed on a 3rd generation dual-source CT system using ATCM in z-axis direction. Images were reconstructed using both, FBP and IR (level 1–5). A Monte-Carlo-simulation-based analysis was used to compare organ-specific-radiation dose. Subjective image quality for various anatomic structures was evaluated using a 4-point Likert-scale and objective image quality was evaluated by comparing signal-to-noise ratios (SNR).
Results: Spiral cCT led to a significantly lower ($p < 0.05$) organ-specific-radiation dose in all targets including eye lense. Subjective image quality of spiral cCT datasets with an IR reconstruction level 5 was rated significantly higher compared to the sequential cCT acquisitions ($p < 0.0001$). Consecutive mean SNR was significantly higher in all spiral datasets (FBP, IR 1–5) when compared to sequential cCT with a mean SNR improvement of 44.77% ($p < 0.0001$).
Conclusions: Spiral cCT combined with ATCM and IR allows for significant-radiation dose reduction including a reduce eye lens organ-dose when compared to a tilted sequential cCT while improving subjective and objective image quality.

1. Introduction

Cranial computed tomography (cCT) is the first-line imaging modality in acute neurological emergencies. Non-contrast enhanced cCT is widely available on a 24/7 basis, quick and easy to perform and provides useful prognostic information in patients with acute ischemic stroke. Moreover, using the ASPECTS template allows physicians to estimate the size of a baseline infarct [1]. Thus, all five large recently published clinical trials that demonstrated the efficacy of endovascular treatment with mechanical devices in patients with acute ischemic stroke used non-contrast enhanced cCT as a first-line imaging tool in the vast majority of patients [2–7].

Abbreviations: ATCM, automated tube current modulation; ASPECTS, Alberta Stroke Program Early CT score; cCT, cranial computed tomography; DSCT, dual-source computed tomography; FBP, filtered back projection; ICRP, International Commission on Radiological Protection; MDCT, multi-detector computed tomography; NC, caudate nucleus; ND, normally distributed data; NI, non-inferiority analysis; HU, hounsfield units; IR, iterative image reconstruction; SNR, signal-to-noise ratios; cCT, cranial CT; WM, white matter.

* Corresponding author at: Department of Neuroradiology, University Medical Center Mannheim, Medical Faculty Mannheim, Heidelberg University, Theodor-Kutzer-Ufer 1-3, 68167 Mannheim, Germany.
E-mail address: Holger-Wenz@gmx.de (H. Wenz).

http://dx.doi.org/10.1016/j.ejro.2016.05.006

The ASPECTS Study Group still prefers sequential scanning in acute stroke patients [8].

Sequential or incremental cCT and spiral or helical cCT are two competing acquisition techniques used for cCT. While spiral CT has mainly replaced sequential CT for most body areas (e.g. abdominal-, thoracic and musculoskeletal-imaging) [9,10], there is still skepticism regarding image quality of spiral cCT [11,12]. Main subjects of skepticism associated with spiral cCT include: inferior delineation of structures with low contrast differences (e.g. grey vs white matter), pronounced beam hardening artifacts localized close to the skull which may mimic hemorrhage [11], as well as lacking demand for rapid brain scanning due to low occurrence of respiration related motion artifacts [12]. However, based on our and otherís experience, there is an enormous demand for shortened cCT acquisition times, especially in agitated patients with acute neurological disorders (e.g. cerebral ischemia or hemorrhage) [13]. Moreover, iterative reconstruction (IR) techniques have shown to improve image quality of cCT when compared to filtered back projection (FBP) independently from the used acquisition technique [14]. Thus, IR techniques may help to overcome previously descripted limitation of spiral CT for gray and white matter differentiation [15]. From a radiation dose perspective, spiral cCT has the advantage that the tube current can be modulated in the z-axis direction of the patient whereas sequential cCT is performed with a fixed tube current over the whole brain.

The aim of this prospective study was to intra-individually compare organ-specific-radiation dose and diagnostic image quality between spiral cCT combined with automated tube current modulation in z-axis direction and IR with sequential cCT without tube current modulation and FBP for image reconstruction.

2. Materials and methods

This prospective single-center study was approved by the institutional review board (IRB) and complies both with the Declaration of Helsinki and the Health Insurance Portability and Accountability Act (HIPAA). All patients provided written informed consent after reading the study information form and additional questions were fully explained by the investigators.

2.1. Patient cohort

31 patients (mean age 67.0 years ±15.5 years [range 28–94 years]; 20 male) with a clinical indication for a non-contrast enhanced cCT and an available previous cCT examination performed at our institution over the last 12 month were prospectively enrolled in this study (12/2013–08/2014). Both inpatients and outpatients were included. Table 1 summarizes the indications for the cCT examinations.

2.1.1. CT acquisition and image reconstruction

The initial clinical routine cCT examinations within the previous 12 months that yielded as the inclusion criteria were all performed on a 4-slice MDCT system (SOMATOM Volume Zoom, Siemens Healthcare Sector, Forchheim, Germany) using a standard sequential technique with the following scan parameters: 120 kVp tube voltage; fixed 270 mAs tube current time product; 4 × 1 mm detector collimation; cranio-caudal scan direction. CT raw data was reconstructed with a slice thickness of 4 mm using FBP and a dedicated brain tissue convolution kernel (H40s medium, Siemens Healthcare Sector, Forchheim Germany).

The prospectively acquiered spiral cCT acquisitions of all patients were performed on a 3rd generation DSCT system (Somatom FORCE, Siemens Healthcare Sector, Forchheim, Germany) using the following scan parameter: 120 kV tube voltage, 330 ref. mAs using automated tube current modulation (ATCM) in z-axis direcetion, 2 × 96 mm detector collimation, 1 s rotation time, pitch factor 0.55; cranio-caudal scan direction. Since the DSCT system does not allow for tilting the gantry the patients were positioned into a dedicated head cup in order to exclude the orbita from the scan field. The CT raw data of the spiral DSCT examinations was reconstructed with a slice thickness of 4 mm using FBP with the corresponding brain tissue convolution kernel (Hr38, Siemens Healthcare Sector, Forchheim Germany). In addition to the FBP reconstructions 5 datasets were reconstructed with a slice thickness of 4 mm using a 3rd generation IR technique (ADMIRE, Siemens Healthcare Sector, Forchheim, Germany) with IR strength levels from 1 to 5.

Table 1
Patient demographics, clinical characteristics and image parameters.

No. of patients	31
Mean age (SD), y	67.0 (15.5)
Range	28–94
Sex, male:female	1.8:1
Indications for scanning, No. of patients	
(Rule out) hemorrhage	12
Follow-up after surgery	7
(Rule out) hydrocephalus	6
Follow-up after cSDH	7
Stroke	6
Trauma	2
(Rule out) abscess	1
CT acquisition	
MDCT	
Data acquisition	sequential
Gantry tilting	yes
Scan direction	cranio-caudal
Detector collimation, mm	4 × 1
Reference mAs	330
Mean CTDIvol, mGy	64.5
Mean DLP, mGy cm	905.3
Pitch factor (ratio)	–
DSCT	
Data acquisition	spiral
Gantry tilting	no
Scan direction	cranio-caudal
Detector collimation, mm	2 × 96 × 0.6
Rotation time, s	1
Mean CTDIvol, mGy	41.8
Mean DLP, mGy*cm	681.5
Pitch factor (ratio)	0.55

CTDIvol = volume computed tomography dose index; DLP = dose-length product; mAs = milliampere-second; *Note*: Some patients had multiple indications for cCT.

2.1.2. Organ-specific-radiation dose

A Monte-Carlo-simulation-based analysis Platform (Radimetrics™, Bayer Healthcare) was used to compare the organ-specific-radiation dose between the two CT techniques. Targets of the comparison were the brain, eye lense, ICRP103, salivary glands and thyroid gland. Additional to the pairwise comparison *t*-test, a non-inferiority analysis was performed. The non-inferior margin was set at 5% upon the mean MDCT organ dose.

2.2. Assessment of objective and subjective image quality

All cCT datasets were transferred to an image viewing workstation (Aycan Osirix Pro, Aycan Digitalsysteme GmbH, Wuerzburg, Germany). Objective image quality was assessed in two predefined anatomic regions by placing identical regions of interest (ROIs) – white matter (WM) and caudate nucleus (NC), excluding pathology that could affect results (e.g. foreign bodies, blood products).

Within the ROIs one radiologist (H.W.) measured image noise, defined as the standard deviation of the measured Hounsfield units (HU), and the mean attenuation (signal) HU.

Table 2
4-Grade scoring system of the subjective evaluation parameters.

Structure	Score 1	Score 2	Score 3	Score 4
Gray/white matter differentiation	Perfect differentiation	Very good differentiation	Delineation not perfect but acceptable for diagnostic purboses	Differences just depictable
Anterior/posterior part of internal capsule	Perfect delineation well-defined anatomy	Very good visualization, well-defined anatomy	Unsharp borders but different structures already visible	Visualization just possible
Subjective image noise	Little to no noise	Optimum noise	Noisy, but permits evaluation	Noisy, degrades image so that no evaluation possible
Ventricular system	Perfect delineation well-defined anatomy	Very good visualization, well-defined anatomy	Unsharp borders but different structures already visible	Visualization just possible
Subarachnoid space	Perfect delineation well-defined anatomy	Very good visualization, well-defined anatomy	Unsharp borders but different structures already visible	Visualization just possible
Infra- and supratentorial artifacts	Free of visible artifacts	Some artifacts but quality not substantially impaired	Substantial decrease in image quality	Image beeing totally impaired by artifacts
Cerebellar hemisphere	Perfect delineation well-defined anatomy	Very good visualization, well-defined anatomy	Unsharp borders but different structures already visible	Visualization just possible
Brainstem	Perfectly visible structure	Good but not perfect	Visible but not in detail	No anatomic detail
Brain lesions (e.g. Lacunar infarct)	Perfectly visible structure	Good but not perfect	Visible but not in detail	No anatomic detail

The signal-to-noise (SNR) ratio was calculated using these measurements. Subjective image quality was independently rated by one experienced neuroradiologist (H.W.) and one experienced radiologist (T.H.), working independently and blinded to the reconstruction method. Evaluation parameters/criteria were as follows: grey/white matter differentiation, delineation of anterior/posterior part of internal capsule on both sides, evaluation of subjective image noise and artifacts, delineation of ventricular system, subarachnoid space, brainstem, cerebellar hemisphere and brain lesions (if present). The subjective image criteria and 4-point-Likert-scale [16] used are summarized in Table 2. The best of all five IR images was identified and compared to sequential cCT images.

Table 3
Calculated organ-specific radiation dose.

Target	Mean [mSv]		SD		Non-inferior analysis		t-test	
	DSCT	MDCT	DSCT	MDCT	*t*-value	*p-value*	*t-value*	*p-value*
Brain	35,6	58,8	5,4	12,3	10,63	<0,0001	9,4	**<0,0001**
Eye lense	51,1	82,3	5,1	16,6	11,13	<0,0001	9,83	**<0,0001**
ICRP103	1,5	2,5	0,26	0,75	7,87	<0,0001	7	**<0,0001**
Salivatory gland	35,6	58,8	5,4	12,3	10,63	<0,0001	9,4	**<0,0001**
Thyroid gland	3,99	6,9	0,82	6,63	2655	0,0051	2,37	**0,0243**

Non-inferiority (NI) analyses were performed at a level of 0.025 (i.e. 95% CI). NI margin was set at 5% of the mean MDCT organ dose.

2.3. Statistical analysis

Statistical analyses were performed using GraphPad Prism 6 (GraphPad Software Inc., La Jolla, CA, USA). We tested for normal distribution using D'Agostino-Pearson normality test. If not indicated otherwise, normally distributed data (ND) are presented as mean ± standard deviation (SD). We performed two-way repeated measures ANOVA analysis to compare objective image quality (i.e. SNR data of WM and NC) across devices and iteration levels with multiple pairwise comparisons using paired *t*-tests, significance threshold was adjusted using the conservative Bonferroni correction. The subjective scoring results were compared using Friedman's test in combination with Dunn's multiple comparison test. The IR method with the highest mean SNR and best subjective image quality was chosen and subsequently compared with the sequential cCT images using Wilcoxon matched paired test. Organ-specific-radiation doses were calculated using Monte-Carlo-simulation in the dedicated software platform and compared between devices using pairwise *t*-test. Additionally we applied a non-inferiority (NI) analysis at an α-level of 0.025 (i.e. 95% CI) using one-sided *t*-test with the NI margin set at 5% of the mean MDCT organ dose. P-values <0.05 were considered statistically significant.

3. Results

All 62 cCT studies were successfully conducted and demonstrated diagnostic image quality at 4 mm. Patient demographics, clinical characteristics, and image parameters are summarized in Table 1.

3.1. Organ-specific dose

The organ-specific dose, calculated by the analysis software, was significantly lower in the spiral cCT acquisitions as shown in Table 3. The brain-, eye lense-, ICRP103- and the salivary gland-doses were significantly lower ($p < 0.0001$) in the spiral cCT. Furthermore a non-inferiority of the spiral cCT acquisitions was shown (Fig. 1).

Table 4
Pairwise comparison of SNR in caudate nucleus in sequential and spiral cCT.

Caudate Nucleus		Sequential	Spiral					
		FBP	FBP	IR1	IR2	IR3	IR4	IR5
Sequential	FBP	1.0	>0.9999	0.1437	<0.0001	<0.0001	<0.0001	<0.0001
Spiral	FBP	> 0.9999	1.0	>0.9999	0.0045	<0.0001	<0.0001	<0.0001
	IR1	0.1437	>0.9999	1.0	>0.9999	0.0035	<0.0001	<0.0001
	IR2	<0.0001	0.0045	>0.9999	1.0	>0.9999	0.0031	<0.0001
	IR3	<0.0001	<0.0001	0.0035	>0.9999	1.0	>0.9999	0.0123
	IR4	<0.0001	<0.0001	<0.0001	0.0031	>0.9999	1.0	>0.9999
	IR5	<0.0001	<0.0001	<0.0001	<0.0001	0.0123	>0.9999	1.0

Note: Significance thresholds were adjusted using Bonferroni correction (n = 21).

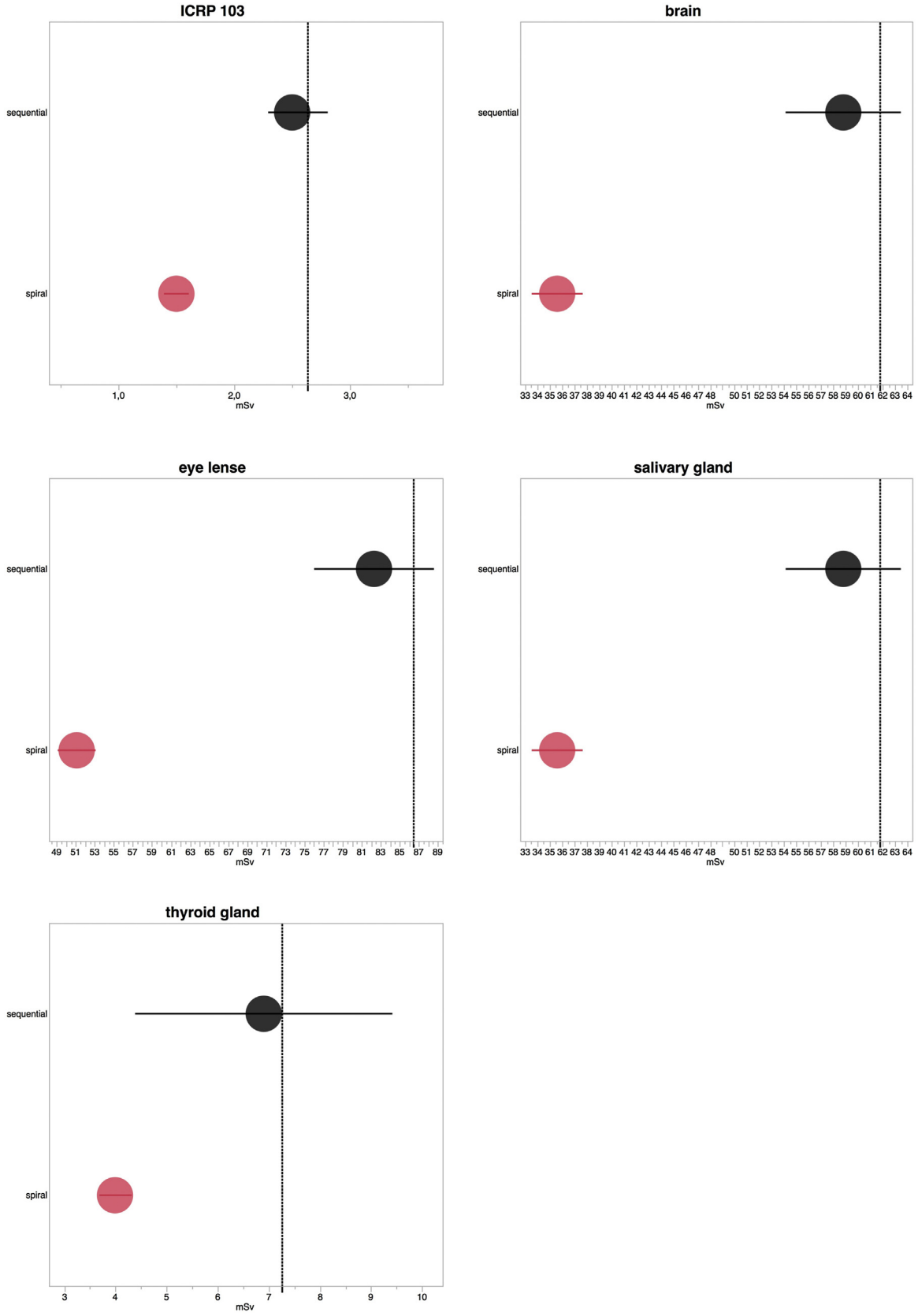

Fig. 1. Non-inferiority analysis; vertical dashed line indicates the non-inferiority margin at 5% upon the mean MDCT organ dose.

Table 5
Pairwise comparison of SNR in white matter in sequential and spiral cCT.

White Matter		Sequential	Spiral					
		FBP	FBP	IR1	IR2	IR3	IR4	IR5
Sequential	FBP	1.0	>0.9999	>0.9999	0.0045	<0.0001	<0.0001	<0.0001
Spiral	FBP	>0.9999	1.0	>0.9999	0.0022	<0.0001	<0.0001	<0.0001
	IR1	>0.9999	>0.9999	1.0	0.7205	0.0035	<0.0001	<0.0001
	IR2	0.0045	0.0022	0.7205	1.0	>0.9999	0.0079	<0.0001
	IR3	<0.0001	<0.0001	0.0035	>0.9999	1.0	>0.9999	0.0232
	IR4	<0.0001	<0.0001	<0.0001	0.0079	>0.9999	1.0	>0.9999
	IR5	<0.0001	<0.0001	<0.0001	<0.0001	0.0232	>0.9999	1.0

Note: Significance thresholds were adjusted using Bonferroni correction (n = 21).

3.2. Quantitative image quality

Comparison between the sequential cCT and all spiral cCT reconstructions showed a significantly superior SNR in the NC (Table 4) and WM (Table 5) ($p_{Bonferroni} < 0.0001$). On the sequential cCT reconstructed with FBP mean SNR in the white matter was 5.63 (±1.15). On spiral cCT, mean SNR of white matter reconstructed with FBP was 6.98 (±1.31).

The mean SNR in the WM increased in the course of higher strength levels of IR as follows: SNR IR 1: 7.19 (±1.39), SNR IR 2: 7.51 (±1.50), SNR IR 3: 7.67 (±1.56), SNR IR 4: 7.88 (±1.64), SNR IR 5: 7.96 (±1.31) (Fig. 2a). The pairwise comparisons using conservative Bonferroni corrections showed a statistically significant higher SNR for higher-compared to lower IR strength levels; similarly, this was also apparent between spiral and sequential cCT (Table 5).

The mean SNR in the NC on sequential cCT reconstructed with FBP was 6.38 (±0.98). Similar to the above-mentioned findings, image noises in the NC decreased and mean SNRs increased with higher strength levels of IR on the spiral cCT acquisitions. SNR of FBP: 8.58 (±1.45), SNR IR 1: 9.17 (±1.74), SNR IR 2: 9.66 (±1.86), IR 3: 10.19 (±1.99), SNR IR 4: 10.75 (±2.17), SNR IR 5: 11.31 (±2.11) (Fig. 2b). The pairwise comparison using Bonferroni correction showed a statistically significant SNR-superiority of higher compared to lower IR strength levels; likewise, this superiority was also apparent between spiral and sequential cCT (Table 4).

In comparison to the sequential cCT acquisitions, ATCM in combination with IR in the spiral cCT acquisitions shows an overall (WM and NC) mean improvement of SNR ratios of 44.77%. Increasing objective image quality is related to higher strength levels of IR; mean improvement (WM and NC) of spiral cCT towards sequential cCT is 29.20% in FBP, 35.72% in IR 1, 42.32% in IR 2, 47.95% in IR 3, 54.17% in IR 4 and 59.27% in IR 5.

3.3. Qualitative image quality assessment

Table 6 shows the mean values of the averaged qualitative ratings per criteria in the nine rated aspects within one reconstruction level reported separately for the two observers.

Mean grading continuously improved within increasing IR strength levels by both readers. In every assessment criteria, the sequential cCT had the worst rating (i.e.: highest score). Moreover, there was a trend to positive correlation that both readers allocated smaller scores (i.e. better readability) for higher strength levels of IR (FBP > IR 1 > IR 2 > IR 3 > IR 4 > IR 5). As a result, IR 5 was rated best by both readers, as evident in all structures (Fig. 3). Consequently IR 5 reconstructions were chosen based on its highest WM- and NC-mean SNR, as well as best subjective image quality profile for pairwise comparison with the spiral cCT (regarding the scoring aspects). Comparing the median scores the IR 5 method had a statistically highly significant better subjective image quality in all examined scoring category than the spiral cCT (Table 7). Figs. 4 and 5 show the direct intra-individual comparison of sequential cCT and spiral cCT.

4. Discussion

The results of our study indicate that spiral cCT with IR and ATCM in z-axis direction leads to superior objective and subjective image quality even with less organ-specific radiation dose including the eye lens when compared to tiled sequential cCT performed without ATCM and FBP reconstructions. The distinct reduction of eye lense radiation dose in the spiral cCT without tilting of the gantry in contrast to the sequential acquisition technique with gantry tilting underscores this superiority and stresses the impact of a dedicated head positioning in order to exclude the orbita from the scan field.

Over the past years, several studies have evaluated IR techniques in various body regions and demonstrated improved diagnostic

Table 6
Mean values of ratings averaged over all examined regions reported separately fort the two observers.

Structure	Mean score (radiologist I) Spiral DSCT						Sequential MSCT	Mean score (radiologist II) Spiral DSCT						Sequential MSCT
	FBP	IR1	IR2	IR3	IR4	IR5		FBP	IR1	IR2	IR3	IR4	IR5	
Gray/white matter differentiation	3,06	2,77	2,19	2.00	1,13	1,03	3,58	2,97	2,52	2,06	2.00	1,65	1,10	3,10
Anterior/posterior part of IC	3,10	2,77	2,29	2,13	1,29	1,06	3,45	3,10	2,90	2,16	2,03	1,32	1,23	3.00
Subjective image noise	3,10	2,81	2,32	2,06	1,23	1,06	3,39	3.00	2,26	2,10	2.00	1,10	1,03	3,32
Ventricular system	3.00	2,77	2,29	2,03	1,26	1,03	3,03	3.00	2,45	2,06	1,97	1,13	1.00	3,13
Subarachnoid space	2,94	2,61	2,29	2,06	1,19	1,03	3,10	3,03	2,35	2,06	1,90	1,03	1.00	3,13
Infra- and supratentorial artifacts	2,48	2,48	2,45	2,42	2,26	2,23	2,74	2,87	2,84	2,81	2,81	2,68	2,68	3,23
Cerebellar hemisphere	3.00	2,48	2,29	2,19	1,71	1,39	3.00	3.00	2,19	2,10	2,03	1,39	1,13	3.00
Brainstem	2,97	2,94	2,58	2,19	1,90	1,58	3,06	3.00	2,87	2,13	2,03	1,87	1,87	3.00
Brain lesions (e.g. lacunar infarct)	3.00	2,74	2,42	2,06	1,52	1,23	3,06	2,97	2,29	2,10	2.00	1,39	1,10	3,06
Cummulative Mean Score	2,96	2,71	2,35	2,13	1,50	1,29	3,16	2,99	2,52	2,18	2,09	1,51	1,35	3,11

IC = internal capsule; *Note*: a smaller score (1–4) represents a better subjective image quality; Only for didactic purposes we present the mean scores. instead of the median scores [12], however the statistical analyses were perfomed using appropriate non-parametrical Wilcoxon matched paired test. IR 5 was chosen for subsequent pairwise comparison with spiral cCT (Table 7).

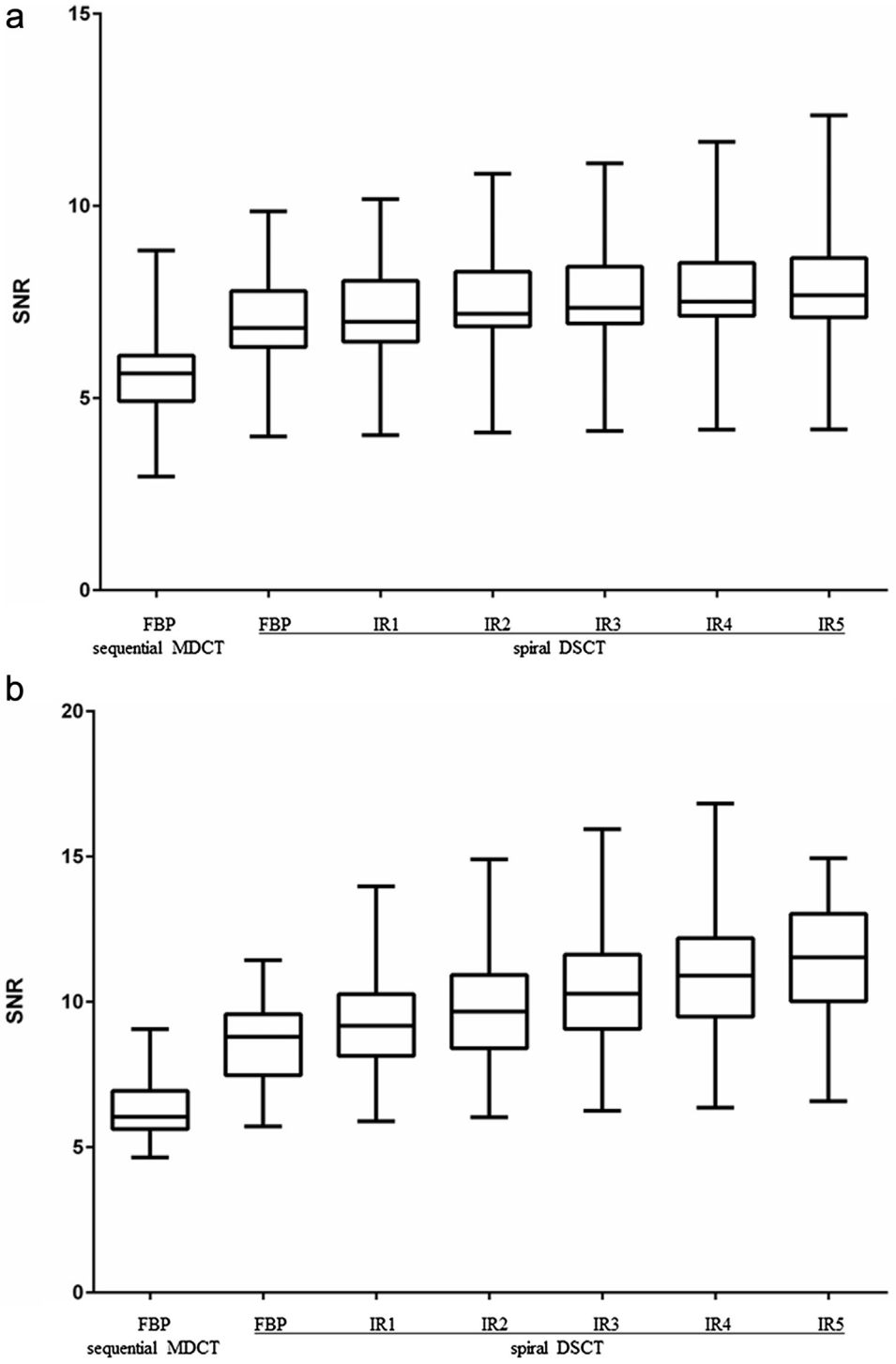

Fig. 2. (a) SNR of FBP and all levels of iterative reconstruction of spiral cCT versus sequential cCT in white matter (WM): there was a highly significant improvement of SNR ($p_{Bonferroni} < 0.0001$). (b) SbNR of FBP and all levels of iterative reconstruction of spiral cCT versus sequential cCT in caudate nucleus (NC): there was a highly significant improvement of SNR ($p_{Bonferroni} < 0.0001$).

image quality and/or reduce radiation dose levels with IR mainly by reducing image noise and image blooming [15,17–20]. However, intra-individual comparison studies between FBP and IR are less available due to ethical reasons that do not allow to scan patients twice. Thus, most studies that showed superiority of IR directly compared FBP and IR reconstructions calculated from the same dataset. The design of our study allowed us to intra-individually compare image quality and radiation dose between standard dose FBP sequential cCT acquisitions and reduced radiation dose iteratively reconstructed spiral cCT datasets. The results of our study are in accordance with other recently published data, that also demonstrated excellent image quality and reduced radiation dose for cCT using a different novel IR technique [21]. Contrary to what one might expect we observed significantly lower eye-lense organ dose values in the spiral cCT acquisitions when compared to our gantry tilted sequential cCT acquisitions. Although, until now, no study intra-individually compared eye lens dose values between both techniques, the majority of radiologists believe that sequential

Table 7
Comparison of spiral iterative reconstruction strength level 5 (IR5) to spiral CT (MSCT).

	Mean score (radiologist I)			Mean score (radiologist II)		
	IR5	Sequential MSCT	P	IR5	Sequential MSCT	P
Gray/white matter differentiation	1.03	3.58	<0.0001	1.1	3.10	<0.0001
Anterior/posterior part of IC	1.06	3.45	<0.0001	1.23	3.00	<0.0001
Subjective image noise	1.06	3.39	<0.0001	1.03	3.32	<0.0001
Ventricular system	1.03	3.03	<0.0001	1.00	3.13	<0.0001
Subarachnoid space	1.03	3.10	<0.0001	1.00	3.13	<0.0001
Infra- and supratentorial artifacts	2.23	2.74	<0.0001	2.68	3.23	<0.0001
Cerebellar hemisphere	1.39	3.00	<0.0001	1.13	3.00	<0.0001
Brainstem	1.58	3.06	<0.0001	1.87	3.00	<0.0001
Brain lesions (e.g. lacunar infarct)	1.23	3.06	<0.0001	1.10	3.06	<0.0001
Cummulative Mean Score	1.29	3.16	<0.0001	1.35	3.11	<0.0001

IC = internal capsule; *Note*: IR series 5 with the highest mean SNR both in gray- and white matter as well with the best subjective image quality was chosen and compared to spiral DSCT images by Wilcoxon sign-rank analysis. Similar to Table 5 mean values are presented because of didactic purposes. Differences are given for both readers.

cCT is generally associated with less radiation exposure to the eye lens. The lower eye lens radiation exposure observed for the spiral cCT acquisitions in our study can be explained by a combination of optimized head positioning in the study population undergoing spiral cCT under study conditions, the use of z-axis based ATCM, the use of IR as well as an optimized full-digital detector technology within the 3rd generation DSCT systems that allows primarily lower applied radiation due to less electronic noise. Thus, our study is not representative for all types of CT systems. State-of-the-art CT systems that allow gantry tilted sequential cCT acquisitions as well as IR may also lead to significantly lower eye-lens radiation exposure.

In the past, there was skepticism against spiral cCT and IR, sometimes leading to low acceptance in routine neuroradiological examinations based on valid objections [11,12]. Therefore, several arguments were marshalled: first, some studies characterized the subjective image quality as unfamiliar or frequently described images as “waxy” or “plastic” when using IR techniques [14,22–26]. Evaluating the subjective image quality, we addressed this phenomenon indirectly. As our results suggest, this phenomenon does

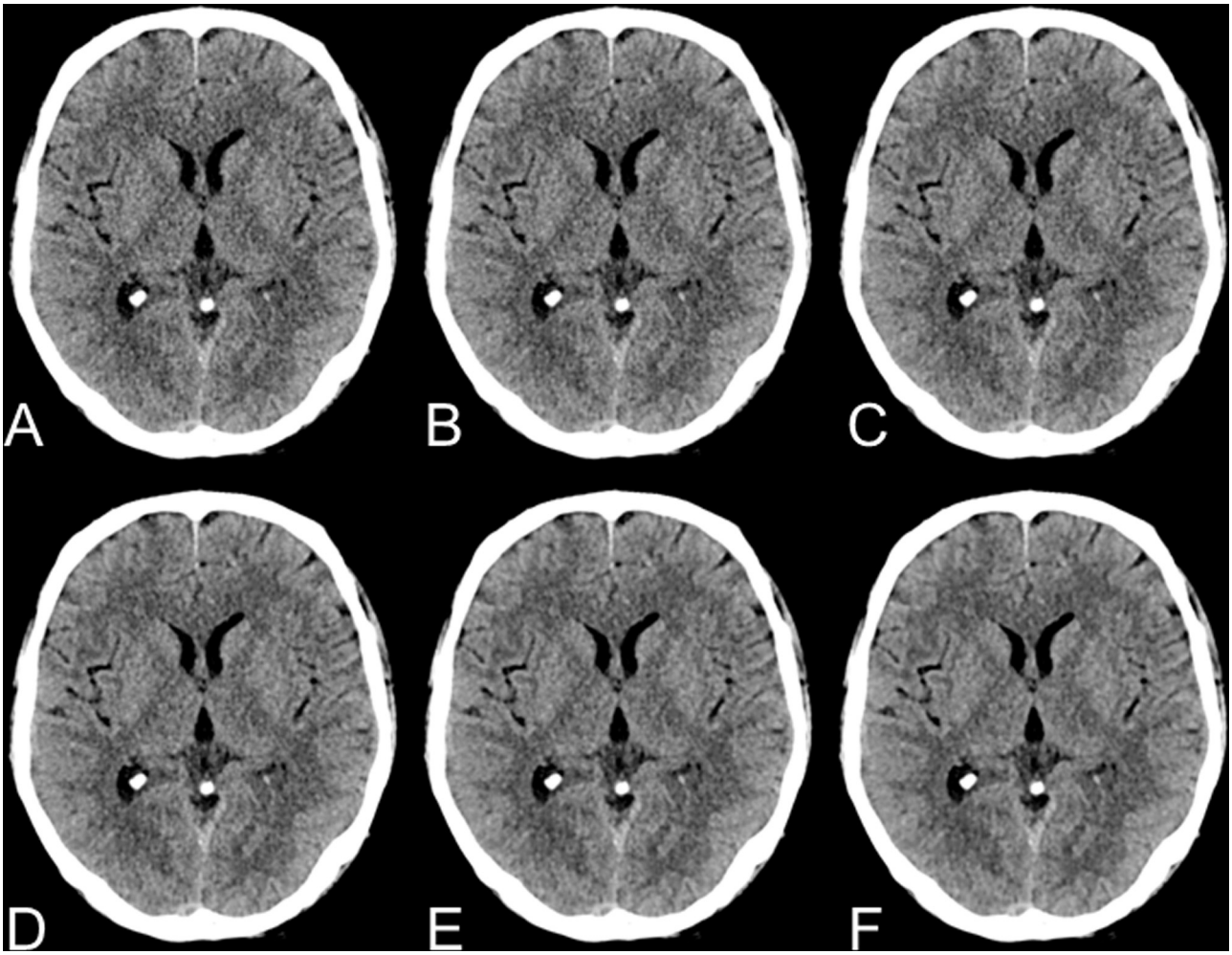

Fig. 3. Cranial CT of a 51-year-old male patient after traumatic brain injury in spiral acquisition mode of a DSCT, using FBP and IR algorithm at 5 different IR strength levels: *A* = FBP, *B* = IR 1, *C* = IR 2, *D* = IR 3, *E* = IR 4, *F* = IR 5.

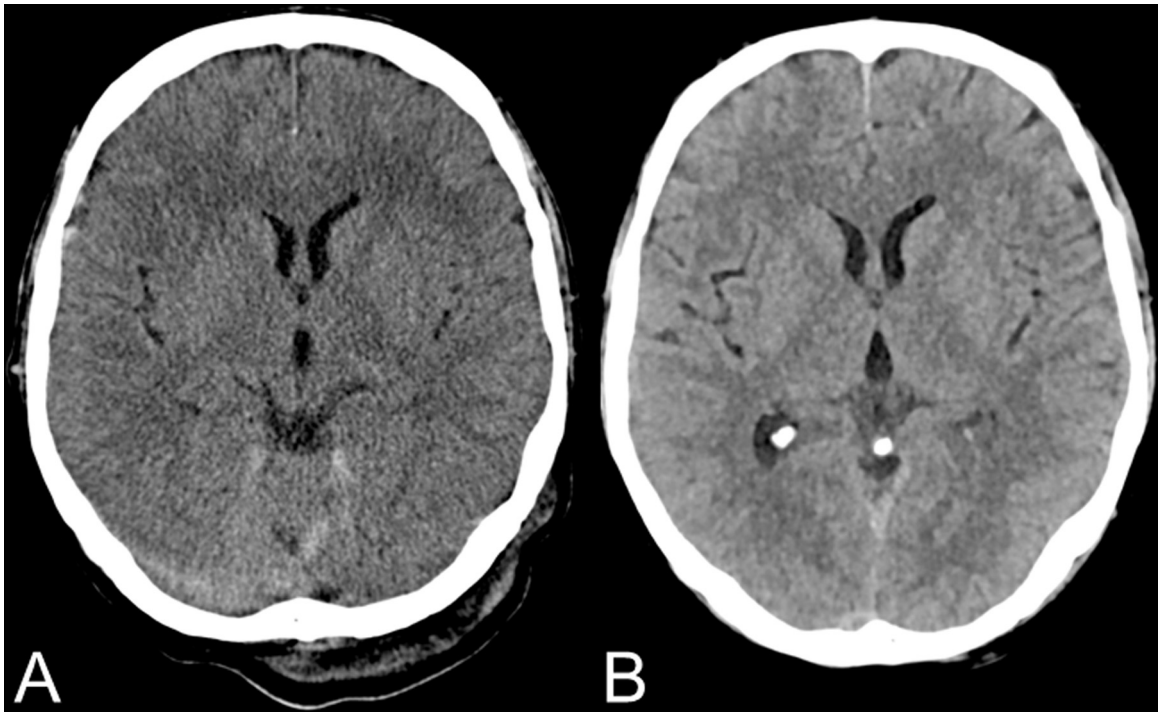

Fig. 4. Intra-individual comparison between cranial CT in a sequential (*A*) and a spiral acquisition mode (*B*) (IR 5). IR 5 was rated best by both readers in all subjective evaluation parameters (*B*).

not constitute as significant detrimental factor, which is likely to be compensated by the reduced noise, among other improvements. However, one has to acknowledge that IR techniques have also improved over the last years and that the first generation IR techniques honestly more suffered from a "waxy" or "plastic" like appearance when compared to the technique evaluated in this study. Second, previous studies encountered artifacts close to the skull in spiral cCT [11], which could be mistaken for acute hematoma or subarachnoidal bleeding. The likely reasons thereof are the physics of linear interpolation which are required for spiral

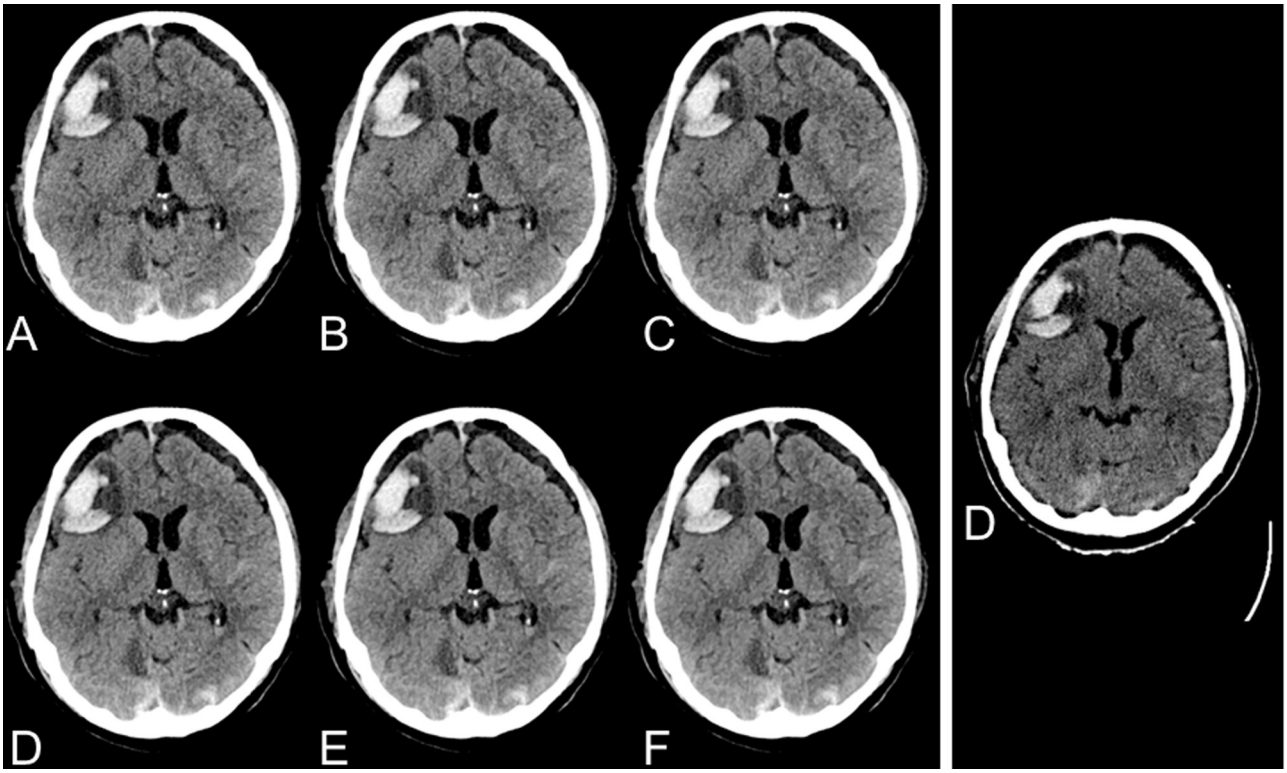

Fig. 5. Cranial CT of a 69-year-old male patient after traumatic brain injury and consecutive intracerebral hemorrhage contusion as well as chronic bilateral subdural hemorrhage. Intra-individual comparison of spiral DSCT at 5 different IR strength levels (*A* = FBP, *B* = IR 1, *C* = IR 3, *D* = IR 4, *E* = IR 5) and sequential MDCT using FBP (*D*).

cCT data processing [27]. However, when using the 3rd generation DSCT and current IR, the occurrences of artifacts significantly decrease. This is crucial in the daily neuroradiological setting, because it enhances the precise differentiation between artifacts and acute hemorrhage in patients with ischemia within the timeframe of thrombolysis [28,29]. Third, it was objected [11] that the delineation of structures with low contrast differences might be inadequate. However, our findings show that the delineation of such structures significantly improves when using spiral cCT aided by advanced IR. Furthermore, the subjective image quality of the spiral cCT datasets was significantly enhanced compared to the standard sequential cCT datasets (all adjusted $p < 0.05$). However, it is to note that IR 5 with the best mean SNR both in WM and NC as well as qualitative image evaluation had the highest variance for WM among all techniques (see Fig. 2a/b). Furthermore, IR has the ability to reconstruct thinner slices which enables to create multiplanar reconstructions more easily [14,30]. Lastly, it has been argued that there is low demand for rapid brain and spine scanning as there are less motion artifacts due to respiration [12]. This, however, is only true for some cases. In polytraumatized patients, some authors favor rapid scanning using spiral cCT [13]. Moreover, especially in a neuroradiological point of view, rapid scanning is beneficial for agitated patients with neurological disorders such as intracranial hemorrhage or cerebral ischemia.

The present study has some limitations that has to be considered. First, this clinical study is of moderate patient size. However, due to our inclusion criteria we aimed to solely include patients with an available sequential cCT within the last 12 months to guarantee intra-individual comparability. Second, the sequential cCT studies were acquiered on a relatively old CT system. Nevertheless, this system is still widely in use for brain CT acquisitions.

In conclusion, spiral cCT in combination with state-of-the-art IR techniques has significant advantages over sequential CT techniques and therefore is likely to pave the way for the implementation of spiral CTs in cranial neuroradiology as a standard procedure. Moreover, the significant reduction in radiation dose levels including the lense will benefit the patients substantially.

5. Conclusion

Spiral cCT in combination with state-of-the-art IR techniques has significant advantages over sequential cCT techniques and therefore is likely to pave the way for the implementation of spiral CTs in cranial imaging.

Conflict of interests

None.

Acknowledgments

This research project is part of the Research Campus M^{2}OLIE and funded by the German Federal Ministry of Education and Research (BMBF) within the Framework “Forschungscampus: public-private partnership for Innovations” under the funding code 13GW00926.

References

[1] P.A. Barber, A.M. Demchuk, J. Zhang, et al., Validity and reliability of a quantitative computed tomography score in predicting outcome of hyperacute stroke before thrombolytic therapy: ASPECTS Study Group. Alberta Stroke Programme Early CT Score, Lancet 355 (2000) 1670–1674.
[2] O.A. Berkhemer, P.S. Fransen, D. Beumer, et al., A randomized trial of intraarterial treatment for acute ischemic stroke, N. Engl. J. Med. 372 (2015) 11–20.
[3] B.C. Campbell, P.J. Mitchell, T.J. Kleinig, et al., Endovascular therapy for ischemic stroke with perfusion-imaging selection, N. Engl. J. Med. 372 (2015) 1009–1018.
[4] M. Goyal, A.M. Demchuk, B.K. Menon, et al., Randomized assessment of rapid endovascular treatment of ischemic stroke, N. Engl. J. Med. 372 (2015) 1019–1030.
[5] T.G. Jovin, A. Chamorro, E. Cobo, et al., Thrombectomy within 8 hours after symptom onset in ischemic stroke, N. Engl. J. Med. 372 (2015) 2296–2306.
[6] B.K. Menon, M. Goyal, Imaging paradigms in acute ischemic stroke: a pragmatic evidence-based approach, Radiology 277 (2015) 7–12.
[7] J.L. Saver, M. Goyal, A. Bonafe, et al., Stent-retriever thrombectomy after intravenous t-PA vs: t-PA alone in stroke, N. Engl. J. Med. 372 (2015) 2285–2295.
[8] ASPECTS Study Group (2016, March 3) Scan protocol. Retrieved from http://www.aspectsinstroke.com/scan-parameters/our-protocol-for-ncct-head-scans/.
[9] J.P. Heiken, J.A. Brink, M.W. Vannier, Spiral (helical) CT, Radiology 189 (1993) 647–656.
[10] R.K. Zeman, S.H. Fox, P.M. Silverman, et al., Helical (spiral) CT of the abdomen, AJR Am. J. Roentgenol. 160 (1993) 719–725.
[11] M.L. Bahner, W. Reith, I. Zuna, et al., Spiral CT vs incremental CT: is spiral CT superior in imaging of the brain, Eur. Radiol. 8 (1998) 416–420.
[12] R. Kuntz, M. Skalej, A. Stefanou, Image quality of spiral CT versus conventional CT in routine brain imaging, Eur. J. Radiol. 26 (1998) 235–240.
[13] A. Reichelt, C. Zeckey, F. Hildebrand, et al., Imaging of the brain in polytraumatized patients comparing 64-row spiral CT with incremental (sequential) CT, Eur. J. Radiol. 81 (2012) 789–793.
[14] H. Haubenreisser, C. Fink, J.W. Nance Jr., et al., Feasibility of slice width reduction for spiral cranial computed tomography using iterative image reconstruction, Eur. J. Radiol. 83 (2014) 964–969.
[15] J.H. Buhk, A. Laqmani, H.C. von Schultzendorff, et al., Intraindividual evaluation of the influence of iterative reconstruction and filter kernel on subjective and objective image quality in computed tomography of the brain, Fortschr Röntgenstr: Fortschritte auf dem Gebiete der Rontgenstrahlen und der Nuklearmedizin 185 (2013) 741–748.
[16] H. Wenz, M.E. Maros, M. Meyer, et al., Image quality of 3rd generation spiral cranial dual-source CT in combination with an advanced model iterative reconstruction technique: a prospective intra-individual comparison study to standard sequential cranial CT using identical radiation dose, PLoS One 10 (2015) e0136054.
[17] B. Bodelle, E. Klein, N.N. Naguib, et al., Acute intracranial hemorrhage in CT: benefits of sinogram-affirmed iterative reconstruction techniques, AJNR Am. J. Neuroradiol. 35 (2014) 445–449.
[18] K. Lahiji, S. Kligerman, J. Jeudy, et al., Improved accuracy of pulmonary embolism computer-aided detection using iterative reconstruction compared with filtered back projection, AJR Am. J. Roentgenol. 203 (2014) 763–771.
[19] C. Ozdoba, J. Slotboom, G. Schroth, et al., Dose reduction in standard head CT: first results from a new scanner using iterative reconstruction and a new detector type in comparison with two previous generations of multi-slice CT, Clin. Neuroradiol. 24 (2014) 23–28.
[20] R.A. Takx, U.J. Schoepf, A. Moscariello, et al., Coronary CT angiography: comparison of a novel iterative reconstruction with filtered back projection for reconstruction of low-dose CT-initial experience, Eur. J. Radiol. 82 (2013) 275–280.
[21] S. Notohamiprodjo, Z. Deak, F. Meurer, et al., Image quality of iterative reconstruction in cranial CT imaging: comparison of model-based iterative reconstruction (MBIR) and adaptive statistical iterative reconstruction (ASiR), Eur. Radiol. 25 (2015) 140–146.
[22] T. Henzler, M. Hanley, E. Arnoldi, et al., Practical strategies for low radiation dose cardiac computed tomography, J. Thorac. Imaging 25 (2010) 213–220.
[23] A. Moscariello, R.A. Takx, U.J. Schoepf, et al., Coronary CT angiography: image quality, diagnostic accuracy, and potential for radiation dose reduction using a novel iterative image reconstruction technique-comparison with traditional filtered back projection, Eur. Radiol. 21 (2011) 2130–2138.
[24] O. Rapalino, S. Kamalian, S. Payabvash, et al., Cranial CT with adaptive statistical iterative reconstruction: improved image quality with concomitant radiation dose reduction, AJNR Am. J. Neuroradiol. 33 (2012) 609–615.
[25] M. Renker, J.W. Nance Jr., U.J. Schoepf, et al., Evaluation of heavily calcified vessels with coronary CT angiography: comparison of iterative and filtered back projection image reconstruction, Radiology 260 (2011) 390–399.
[26] S. Singh, M.K. Kalra, J. Hsieh, et al., Abdominal CT: comparison of adaptive statistical iterative and filtered back projection reconstruction techniques, Radiology 257 (2010) 373–383.
[27] W.A. Kalender, A. Polacin, Physical performance characteristics of spiral CT scanning, Med. Phys. 18 (1991) 910–915.
[28] W. Hacke, M. Kaste, E. Bluhmki, et al., Thrombolysis with alteplase 3–4.5 hours after acute ischemic stroke, N. Engl. J. Med. 359 (2008) 1317–1329.
[29] R. von Kummer, K.L. Allen, R. Holle, et al., Acute stroke: usefulness of early CT findings before thrombolytic therapy, Radiology 205 (1997) 327–333.
[30] H.C. Becker, D. Augart, M. Karpitschka, et al., Radiation exposure and image quality of normal computed tomography brain images acquired with automated and organ-based tube current modulation multiband filtering and iterative reconstruction, Invest. Radiol. 47 (2012) 202–207.